
Article

Numerical Simulation Prediction of Erosion Characteristics in a Double-Suction Centrifugal Pump

Xijie Song¹, Ning Gu², Yubin Shen², Xiaoming Fan², Zhengwei Wang^{1*}

¹ Tsinghua University. Tsinghua Univ, Dept Energy & Power Engn; wzw@mail.tsinghua.edu.cn.com

² Water conservancy project construction center of Ningxia Hui Autonomous Region; 270698903@qq.com

* Correspondence: wzw@mail.tsinghua.edu.cn; Tel.: (Tsinghua University. Tsinghua Univ, Dept Energy & Power Engn, Beijing 100084, China)

Abstract: Double suction centrifugal pump installed along the Yellow River faces the serious sediment erosion due to the high sediment content which cause the poor operation efficiency of pump unit. The particle motion characteristics and erosion characteristics in the pump under different flow rates and different particle concentrations were numerically simulated based on the particle track model of solid-liquid two-phase flow. The results show that the flow rate has a significant effect on the particle tracks and the erosion caused by the particles in the impeller. The total erosion rate is positively correlated with the flow rate, and increases with the increase of flow rate. The vortex and secondary flow in the impeller have obvious influence on the particle trajectory, which increases the particle concentration at the trailing edge of the pressure surface and intensifies the impact erosion in this area. The particles carried by the vortex intensifies the local erosion. The particle concentration mainly affects the erosion rate, but has little effect on the erosion position. The influence of flow rate on the pump erosion is greater than that of the particle properties. These results provide a reference for optimization of the design of anti-erosion blades of the double-suction pump and regulation-operation of pumping station.

Keywords: centrifugal pump; impeller; erosion; particle track; particle concentration; flow rate

1. Introduction

Double suction centrifugal pump can produce large flow and high head, which is widely used in irrigation pumping stations along the Yellow River [1]. The Yellow River is one of the rivers with the highest sediment concentration in the world, which makes the pumping units from the pumping stations along the Yellow River suffer from serious sediment abrasion, seriously affects the normal operation of pumps, reduces the working efficiency of pumps, and causes huge positive economic losses and energy waste [2].

Up to now, a large number of researches on studying the solid-liquid two-phase flow in centrifugal pumps have been carried out, and in-depth researches on the erosion and damage on the parts of the flow passage of centrifugal pumps also have been conducted [3-5]. The erosion of different parts in the pump is mainly due to the change of the characteristics of two-phase flow and the characteristics of surface structure material, and the appearances of the damaged surfaces are different [6]. According to the erosion pattern in the pump, the erosion is divided into two basic patterns: general erosion and local erosion. The general erosion is caused by the particles in water flow in the pump scouring the surface of the flow passages [7]. The surface of the material with common erosion presents the same ripple erosion trace, which can clearly reproduce the movement direction of particles. Local erosion is more serious general erosion which happens in some areas of the pump [8]. Local erosion is usually caused by the deterioration of the flow state near the surface of the parts of flow passage [9]. Xu studied the movement of solid particles in a centrifugal pump impeller by using high-speed photography technology, and found that the particle size, the impeller speed, and the blade angle all have a significant effect on the

movement of the particles [10]. Liu [11] found that the characteristics of discrete particles and impeller speed have important influence on both the trajectory of solid particles and the process of wall collision by tracking the particle trajectory in solid-liquid flow field. Qian found that the blade erosion rate is related to velocity and impact angle through numerical simulation of different blade inlet edge shapes [12]. K.C. Wilson et al. found that the main erosion mechanisms that cause pump erosion can be divided into sliding erosion and impact erosion, depending on the impact angle of the particles along the pump geometry [13]. Xu studied the flow in solid-liquid pump and found that the flow pattern of solid-liquid two-phase flow in solid-liquid pump is closely related to erosion. The better the flow condition in the pump (no large-scale flow separation, local high velocity and large pressure pulsation, the smoother the flow is), the less the degree of erosion in the flow passages [14]. At different stages of the operation life, the erosion rate of solid-liquid pump varies greatly. In the early stage of erosion, the erosion on the flow passage caused by particles is similar to polishing on the surface, and the speed of erosion is slow and the degree of erosion is small. In the stable erosion period, the erosion of the flow passage parts is mainly general erosion, and the degree of the local erosion increases gradually [15]. The erosion causes the deterioration of the flow state in the pump, and then accelerates the local erosion. In the later stage of erosion, the erosion is further accelerated, the material loss of the parts in the flow passages increase more than that of the previous two stages, and cavitation may also be induced. The combination of erosion and cavitation greatly aggravates the damage of the materials until the parts in the flow passage are damaged. When the same slurry is transported by different pumps and different slurry is transported by the same pump, if the operation efficiency of the pump is high, the erosion is uniform [16]. If the operation efficiency of the pump is low, the serious erosion caused by impact and vortex will occur. After the blade outlet is worn, the blade will become thinner. Especially in the root of the hub, the erosion is serious, and the strength of the blade is weakened. Finally, the blade will break because it cannot bear the pressure difference between the pressure surface and the suction surface [17].

The particles are taken as discrete phase and liquid as continuous phase in the particle track model, and particle motion in Lagrange coordinate system and continuous phase motion in Eulerian coordinate system are calculated. Then a large number of particles are counted so that the macro trajectory of particle motion is obtained [18]. The velocity of particles on any trajectory can be obtained by using Lagrange method. Xu used this method to simulate the movement of solid particles in the centrifugal pump, and the predicted results are close to the experimental values [19]. Meanwhile, in order to ensure the reliability of erosion rate prediction, Finnie [20], Tabakoff [21], have proposed different erosion rate prediction models. These empirical models are basically established on the basis of erosion tests, and the actual variables (impact velocity, impact angle and impact frequency) determine the size of these variables in these empirical models. Some studies prove that Tabakoff erosion model is more accurate [23].

In this paper, the erosion of a double suction centrifugal pump along the Yellow River is predicted and analyzed by numerical simulation due to the large seasonal variation of the Yellow River water flow. This paper focuses on the study of particle trajectory and erosion distribution in the impeller of double suction centrifugal pump under different flow rate conditions and different sediment concentrations. Tabakoff erosion model is used to predict the erosion of centrifugal pump. This study is helpful to reveal the mechanism of erosion and solve the problem of erosion damage in engineering.

2. Materials and Methods

2.1 Research object

The research object of this paper is a double-suction centrifugal pump. The main parameters of the entire calculation model are: rated flow $Q_d=3.083\text{m}^3/\text{s}$, rated head $H=50\text{m}$, rated efficiency $\eta_r=86\%$, rotation speed $n=490\text{r}/\text{min}$, number of blades $z_b=16$, impeller

diameter $D=1275\text{mm}$, as shown in figure 1. Figure 2 shows the name of the impeller components.

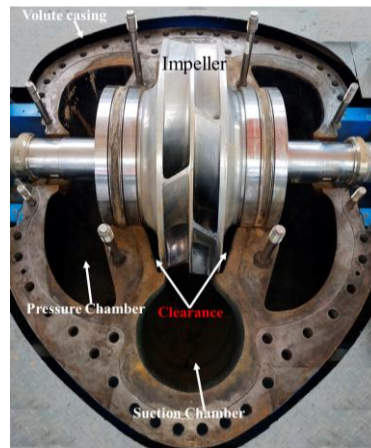


Figure. 1 Centrifugal pump

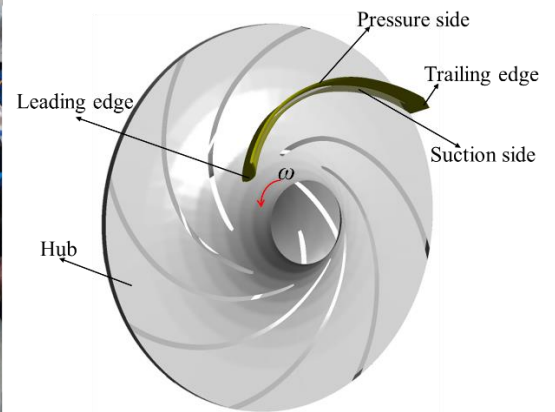


Figure. 2 Impeller components

The calculation model is meshed by the software Workbench, and the unstructured grid and structured grid are used, as shown in figure 3, and the grid independence check is carried out by analyzing the change of head under different the number of grids, as shown in figure 4. When the number of grids reaches 4.21 million, the head basically remains unchanged, so the final number of grids is 4.21 million.

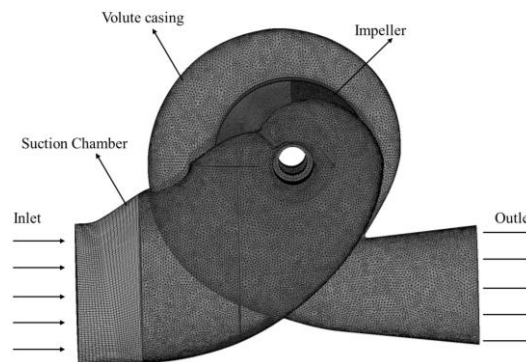


Figure. 3 Grid of the calculation model

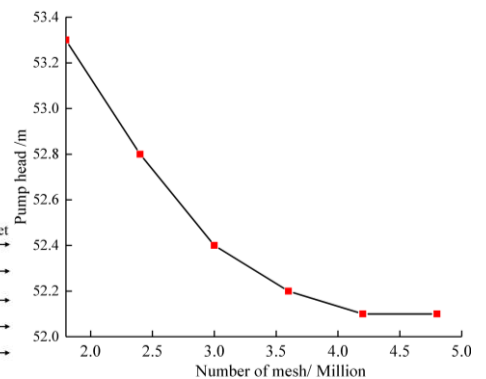


Figure. 4 Change curve of the pump head with grid number

2.2 Basic equation of particle motion

In the Lagrangian framework, when the particles move in the liquid, the force comes from the velocity difference between the particles and the fluid.

The main forces on particles are gravity, resistance, virtual mass force, pressure gradient force, Basset force, Saffman force, Magnus force and so on.

$$m_p \frac{du_p}{dt} = F_D + F_B + F_G + F_V + F_P + F_X \quad (1)$$

Where t is time, m_p is particle mass, u_p is particle velocity, F_D is resistance, F_B is basset force, F_G is gravity, F_V is virtual mass force, F_P is pressure gradient force, F_X is the sum of other external forces considered.

In this paper, the particle concentration in the flow field is small, the fluid velocity of the continuous phase in the pump is large, and there is a large density difference between the continuous phase and the discrete phase. Therefore, the virtual mass force, pressure gradient force, basset force, Saffman force and Magnus force on the solid particles can be ignored. The basic equation of particle motion can be expressed as

$$\frac{dx_{pi}}{dt} = u_{pi} \quad (2)$$

$$\frac{du_{pi}}{dt} = \frac{3C_D \rho_f}{4\rho_p D_p} |u_s| u_s \quad (3)$$

u_s is the slip velocity between particles and liquid, C_D is the drag coefficient related to Reynolds number, ρ_f is the liquid density, ρ_p is the particle density, D_p is the particle diameter, and x_{pi} is the spatial coordinate position of particles. It can be seen from the formula that when the particle moves in the liquid, the particle trajectory is related to the particle diameter and density.

2.3 Erosion model

ANSYS CFX is used to calculate the flow field. The particle track model is used to calculate the flow field. The coupling mode of the calculation model is one-way coupling. Tabakoff erosion model is used to predict erosion. According to the particle track model, each group of particles moves along its own independent trajectory from the initial position, the particles are independent of each other, and there is relative velocity slip between particles and fluid, ignoring the turbulent diffusion, viscosity and heat conduction between particles. Tabakoff erosion model is an empirical and semi empirical erosion model considering the effects of different particle velocities and collision angles on target erosion. The model is based on the impact angle and collision velocity (i.e. particle trajectory) of particle impacting the surface.

$$E = f(\gamma) \left(\frac{V_p}{V_1}\right)^2 \cos^2 \gamma \left[1 - \left(1 - \frac{V_p}{V_3} \sin \gamma\right)^2\right] + \left(\frac{V_p}{V_2} \sin \gamma\right)^4 \quad (4)$$

$$f(\gamma) = \left[1 + k_1 k_{12} \sin\left(\gamma \frac{\pi/2}{\gamma_0}\right)\right]^2 \quad (5)$$

$$k_1 = \begin{cases} 1 & \gamma \leq 2\gamma_0 \\ 0 & \gamma > 2\gamma_0 \end{cases}$$

Here E is the dimensionless mass (mass of eroded wall material divided by the mass of particle). V_p is the particle impact velocity. V_1 , V_2 and V_3 are the parameters of particle impact velocity. γ is the impact angle in radians between the approaching particle track and the wall, γ_0 being the angle of maximum erosion. k_1 , k_{12} and γ_0 are model constants and depend on the particle/wall material combination.

The formula (4) can be divided into two parts: the first is the small angle cutting damage of particles, which is the damage mechanism of particles on the ductile materials; The second is the erosion damage of the target by the normal velocity of particles, which is proportional to the Fourth Square of the velocity, which is the failure mechanism of particles on brittle materials.

Because the erosion model can comprehensively consider the joint effects of ductile materials and brittle materials, it can more comprehensively predict the erosion characteristics. However, due to the large number of empirical coefficients and strong pertinence, the erosion model is mainly suitable for steel, aluminum and other materials.

2.4 Calculation method for solution

The total pressure inlet condition is adopted in the calculation domain, and the volume fraction of particles at the inlet is assumed to be evenly distributed; The total mass flow rate is adopted at the outlet. For the wall in contact with liquid in the parts in the flow passages, the non-slip wall condition is adopted for the fluid phase, the free slip wall condition is adopted for the solid particle phase, and the standard wall function is adopted near the wall. The SST $k-\omega$ was chosen as the turbulence model, the particle track model was used for solid phase, and Tabakoff and Grant Erosion Model was used for erosion model. High precision difference scheme and RMS residual scheme are used to solve the problem, and the accuracy is set to 10^{-5} .

3 Discussion of Calculation Results

3.1 Verification of Calculation Scheme and Reliability

In this paper, the particle motion under different flow rate and concentration was analyzed. In CFX setting, the discrete phase of particles was set as dilute phase, and the collision between particles was not considered. The collision between the particle and the solid wall was assumed completely elastic without considering the energy loss. The characteristics of flow and erosion inside the impeller were analyzed under three typical conditions of $0.25Q_d$, Q_d and $1.27Q_d$.

Table. 1 sediment condition

Parameter	Scheme Number					
	1	2	3	4	5	6
Flow rate(m^3/s)	0.25	Q_d	$1.27Q_d$	Q_d	Q_d	Q_d
particle concentration (kg/m^3)	15	15	15	11	7	1

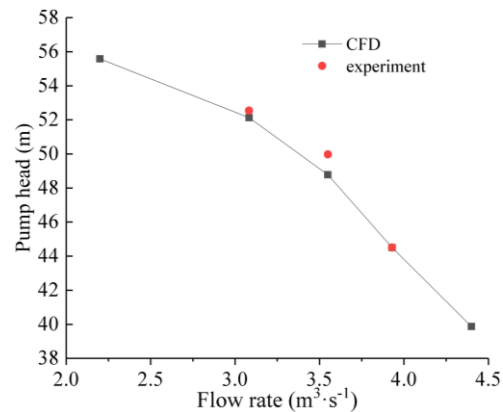


Figure. 5 Change curve of pump efficiency

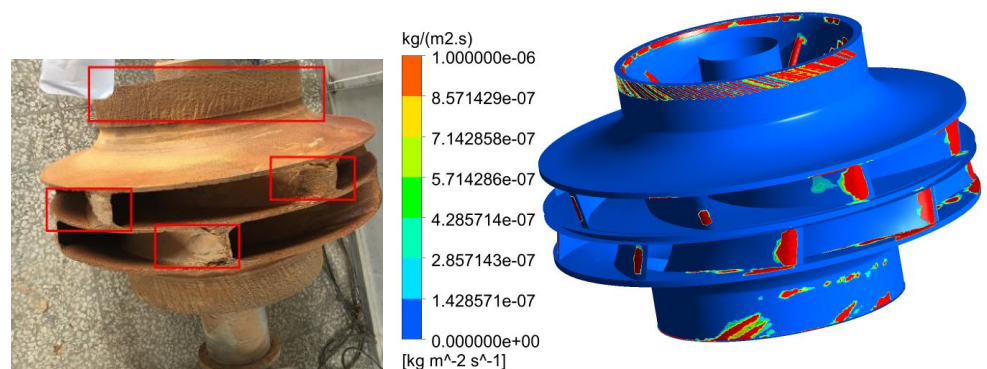


Figure. 6 Physical picture of erosion **Figure. 7** Erosion result of numerical simulation

The energy performance curve of double-suction centrifugal pump is obtained by clear water calculation, as shown in Figure 5. The experimental results are provided by Andritz company. The energy performance obtained by numerical simulation is consistent with the experimental results, and the error is within 0.3%. Fig. 6 is a physical picture of the abrasion of the pump unit of the Yellow River Pumping Station. Figure 7 shows the distribution of erosion rate when the particle inlet particle concentration is $15kg/m^3$ and the particle size is $0.025mm$. In engineering, pump erosion is due to long-term damage caused by different factors. However, numerical simulation is an ideal method to calculate the erosion prediction under a specific condition, and there are inevitably some errors in the predicted erosion results. On the whole, the erosion position and erosion

morphology of the front cover plate wall and the blade outlet pressure surface predicted by the numerical simulation were consistent with the erosion characteristics of the pump impeller in the project site. The calculation results of external characteristics and erosion show that the numerical simulation method is reliable.

3.2 Analysis of flow and erosion in double-suction pumps under different flow conditions

3.2.1 Influence of flow rate on particle movement

In the process of pump operation, it often needs to operate under different flow conditions. The change of flow conditions often leads to the change of flow field structure and particle distribution in the pump. This section focuses on the influence of flow rate on particle trajectory and particle distribution. Figure 8 shows the flow pattern distribution on the surface of impeller cover plate under different conditions when the particle concentration is 15kg/m^3 . Under the condition of small flow rate, the flow pattern in impeller was the worst, and there were different degrees of vortex and secondary flow caused by flow separation in many locations. The multi-scale vortex flow in the blade channel blocks the blade channel, and the junction between the vortex boundary and the blade was the high-speed region. There were frequent frictions between the particles carried by the vortex and the wall. With the increase of flow rate, the uniformity of flow pattern in impeller was obviously improved. Under the two flow conditions of Q_d and $1.27Q_d$, the flow was smooth in the blade channel, and there was no vortex.

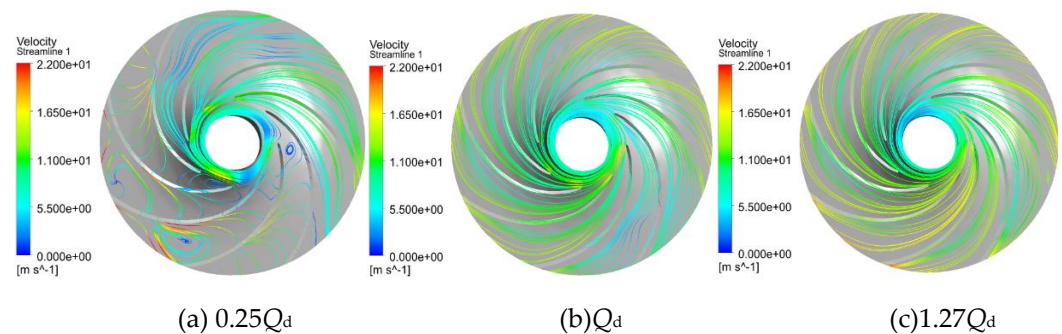


Figure. 8 Flow pattern in impeller under different flow rate conditions(15kg/m^3)

Figure 9 shows the particle distribution in the impeller under different conditions when the particle concentration is 15kg/m^3 . Under the condition of small flow, the particle distribution in the impeller was uneven. With the increase of flow, the uniformity of particle distribution in the impeller increased. However, the number of particles and the relative velocity of particles varied greatly in different blade channels. At the impeller inlet, the particle concentration distribution was the largest, and the number of particles in contact with the impeller inlet was also the largest. The relative velocity of the particles at the tail edge of impeller outlet was the largest under non rated condition (Q_d). The distribution patterns of the particle in impeller were consistent with the changes of the flow states under different flow conditions, which indicates that the flow rate has a great influence on the characteristics of the particle movements.

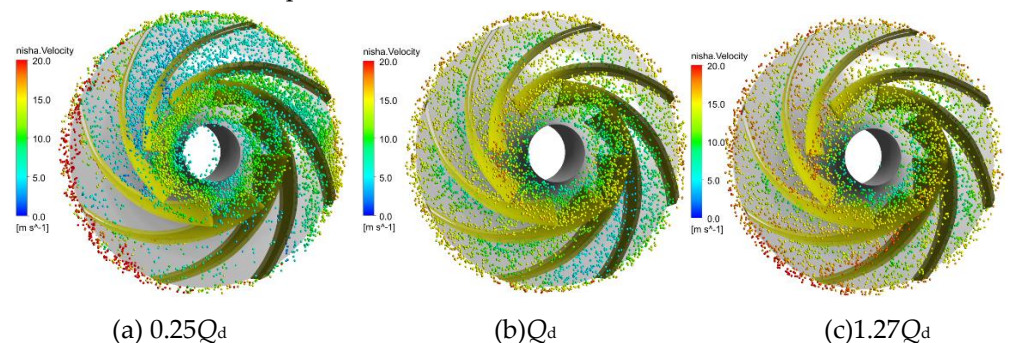


Figure. 9 Particle distribution in impeller under different flow rate conditions(15kg/m^3)

3.2.2 Effect of flow rate on surface erosion

Figure 10 and figure11 show the erosion distribution in the impeller under different working conditions when the particle concentration is 15kg/m^3 . The results show that the erosion distribution and erosion loss of blades and hub on both sides of double suction centrifugal pump are asymmetric. The erosion positions under different flow conditions were obviously different, which was directly related to the distribution position and motion trajectory of particles, indicating that the flow condition directly affected the erosion positions in the impeller. Under the condition of small flow rate, the internal erosion of double suction centrifugal pump mainly included inflow impact erosion, blade channel friction erosion, vortex erosion and blade head impact erosion. With the increase of flow rate, the inflow gradually became uniform, and the inflow impact erosion and vortex erosion disappeared. The internal erosion of impeller was mainly the friction erosion in blade channel and the impact erosion at blade head. And with the increase of flow rate, the erosion range in the blade channel increased gradually, and the characteristics of anti-erosion in the impeller were the best under the rated condition. The larger the flow rate was, the more uniform the particle distribution was, and the smaller the erosion degree on the hub and blade passage wall was, but the greater the particle concentration at the impeller inlet was, the higher the relative velocity was, and the higher the erosion intensity on the blade head was.

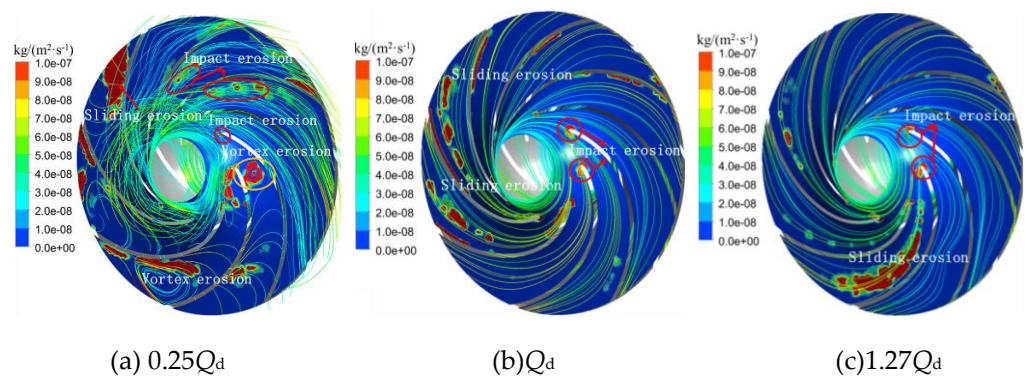


Figure. 10 Erosion distribution of hub under different flow rate conditions(15kg/m^3)

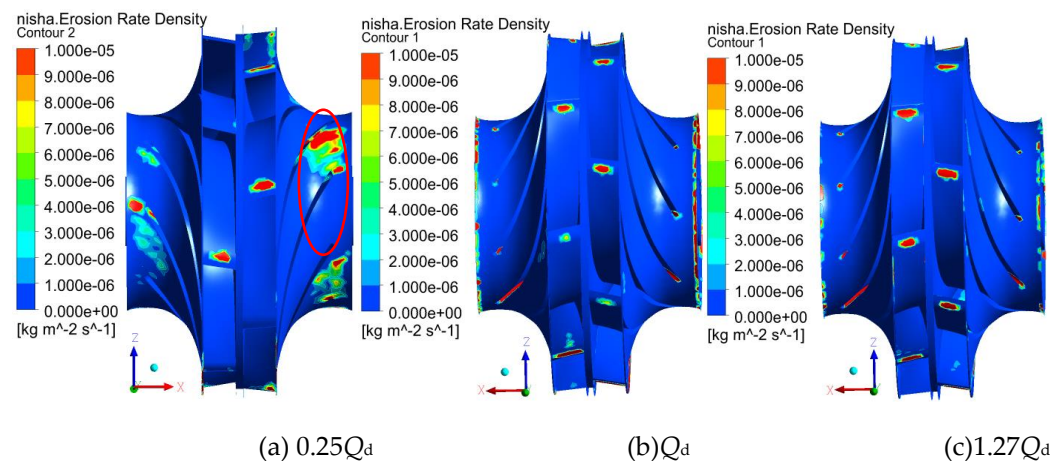


Figure. 11 Distribution of erosion in impeller under different flow rate conditions

Through the analysis, it can be seen that the blade wall and the hub wall were worn under different flow conditions, which belonged to the common erosion caused by flow.

Under the condition of small flow rate, there will be local erosion caused by vortex, and the local erosion caused by vortex was mainly friction erosion. The total erosion rate of inner blade and hub wall under different flow conditions was analyzed quantitatively. Figure 12 and figure 13 show the total erosion rate curves of blade wall and hub wall under different flow conditions. The total erosion rate of blade wall positively correlated

with the flow rate, and increases with the increase of flow rate. The results show that the erosion rate in the impeller is obviously different under different flow conditions, which indicates that the flow condition not only affects the erosion position in the impeller, but also has a great influence on the erosion rate. The results show that there are differences in the variation curves of the wall erosion rate of the blades on both sides, which indicates that the total erosion amount of the blades on both sides is different.

The erosion rate of the hub wall decreases from $0.25Q_d$ to Q_d , and increases from Q_d to $1.27Q_d$. The variation of the erosion rate of the hub wall with the flow condition also shows that the erosion amount on both sides of the double suction centrifugal pump is also different.

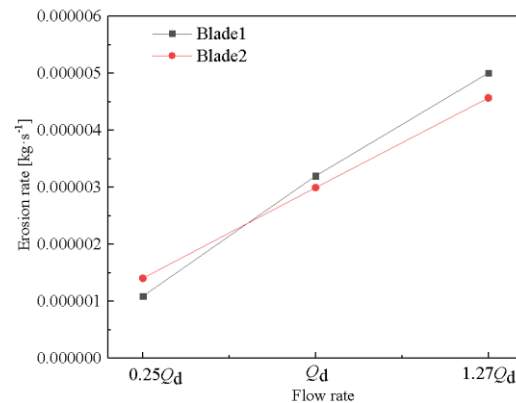


Figure. 12 Erosion rate at blade changes with flow rate

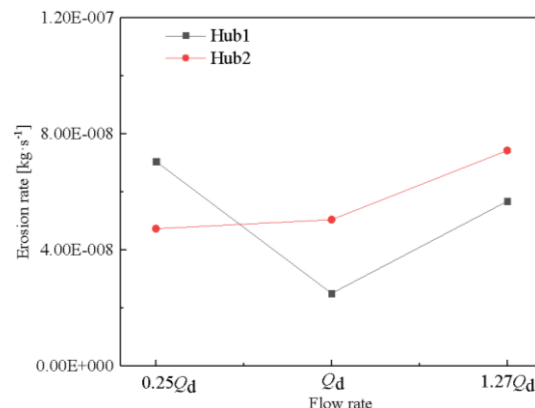


Figure. 13 Erosion rate at hub changes with flow rate

3.2.3 Local erosion caused by vortex in impeller

In this section, the erosion mechanism under the condition of small flow is analyzed, focusing on the vortex structure and the local erosion caused by second flow. Figure 14 shows the three-dimensional structure of vortex in double suction centrifugal pump using Q criterion. Due to the uneven velocity distribution in the impeller blade passage, the vortex attached to the hub and the passage vortex along the blade passage are generated in the impeller. The vortices have a great influence on the particle trajectory. Under the influence of the flow passage vortex, the particle trajectory moves from the suction to the pressure surface in the outlet section of the impeller. Under the influence of passage vortex, the particle concentration on the pressure surface at the outlet of impeller increases, which aggravates the erosion in this area. The particles carried by the local wall attached vortex rub against the wall of the local vortex region, which aggravates the local friction and erosion. Under the condition of small flow rate, the flow field structure in the impeller is unstable and the main flow velocity is relatively low, which leads to the secondary flow in the impeller. Due to the secondary flow in the blade channel, the particles are easier to

separate from the carrier, causing the local velocity increase. With the increase of local velocity, the relative velocity of particles will also increase.

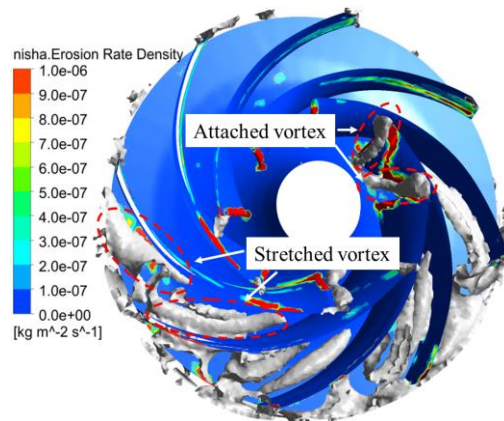


Figure. 14 Vortex structure in double suction centrifugal pump

In addition, compared with the back cover shell, the velocity and vortex intensity near the blade surface are higher, and the particles are easier to impact the blade surface, so the asymmetric corrosion on the blade surface is more obvious. The vortex erosion under small flow conditions is a local erosion, and the vortex rotation speed reflects the vortex rotation intensity and reflects the degree of the local erosion caused by vortex.

According to the previous analysis, the wear degree of the vortex on the wall along the radial direction of the vortex is different, so the relationship between the erosion rate and the radius of the vortex core is used to quantitatively analyze the correlation between the erosion rate and the vortex. The variation curves of the circumferential velocity of vortex core and the surface erosion rate at vortex area with the radius of vortex core is shown in figure 15. The results show that the circumferential velocity of vortex core increases with the increase of vortex core radius, and the maximum circumferential velocity occurs at the maximum vortex core radius. The results show that the erosion rate at the vortex core boundary is the largest, this is because the particle concentration near the vortex core center is low, the particle relative velocity is small, and the erosion rate is small. However, the vortex moves in the impeller passage continuously, and the vortex boundary will be subject to uneven friction of particles carried by the vortex, resulting in local erosion. The greater the radius of vortex core, the greater the rotational speed of vortex and the higher the erosion rate.

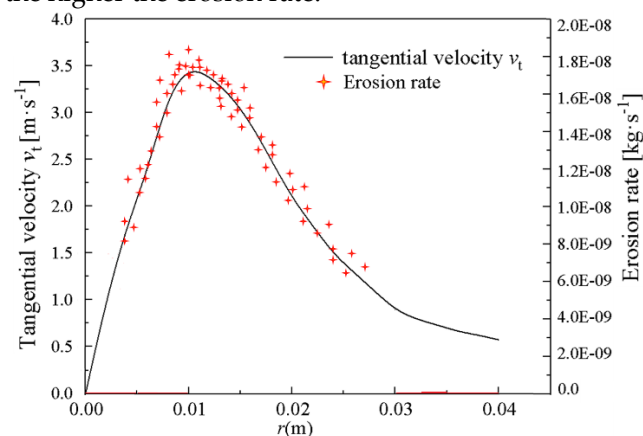


Figure. 15 Circumferential velocity and erosion rate change with vortex core radius

3.3 Effect of particle concentration on erosion characteristics

Generally, the water pump operates in rated condition for a long time. The particle movement trajectory and erosion distribution under different particle concentrations are analyzed to explore the influence of particle concentration on erosion characteristics.

3.3.1 Influence of particle concentration on particle tracks

Figure 16 shows the trajectory of a single particle with different particle concentrations. It can be seen that the change of particle concentration has little effect on the trajectory of particles. This is because the particle size does not change, and its force state does not change. Therefore, when the particle concentration changes, its trajectory will not change significantly.

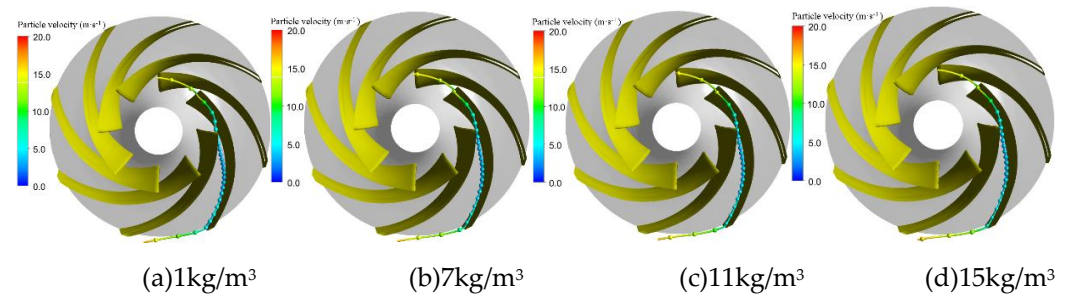


Figure. 16 Trajectory of single particle with different particle concentration

Figure 17 and figure 18 show the particle distribution and solid volume fraction distribution under different particle concentrations, respectively. In the case of the same particle size, the distribution of particles in the centrifugal pump under different particle concentrations does not change obviously, so the particle concentration has little effect on the distribution of particles in the single channel, which is consistent with the description of particle trajectory. After the sediment laden flow enters the impeller, the particles accumulate at the leading edge of the blade. When the particle concentration is 1kg/m^3 , the particle distribution in the impeller is very uniform, and there is a strip of particle aggregation distribution at the impeller inlet. With the increase of particle concentration, particles gather in the outlet direction of the suction surface of the blade passage, and the impact frequency of particles on the blade surface increases. The larger the particle concentration is, the more uneven the particle distribution is in the impeller, and the more serious the particle aggregation is on the suction surface and pressure surface of the blade. Due to the backflow near the tongue of the impeller, the concentration of particles near the tongue increases.

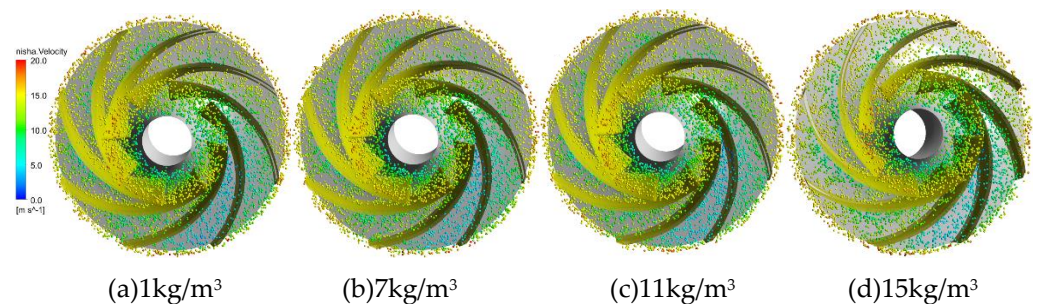


Figure. 17 Particle distribution under different particle concentrations

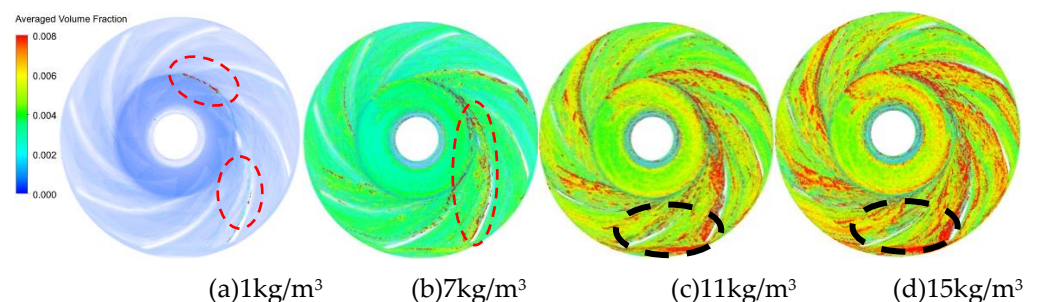


Figure. 18 Distribution of solid volume fraction under different particle concentrations

3.3.2 Effect of particle concentration on erosion characteristics

Figure 19 shows the distribution of single blade erosion rate with different particle concentrations. It can be seen from figure 19 that the erosion rate of leading edge and trailing edge increases with the increase of particle concentration under the same particle size and different particle concentration, and the erosion morphology is the same. It can be seen that the change of particle concentration basically does not change the erosion morphology and erosion position, only changes the erosion range and erosion rate on the original position, which is consistent with the particle motion trajectory, that is, the particle concentration has little effect on the erosion morphology and erosion position.

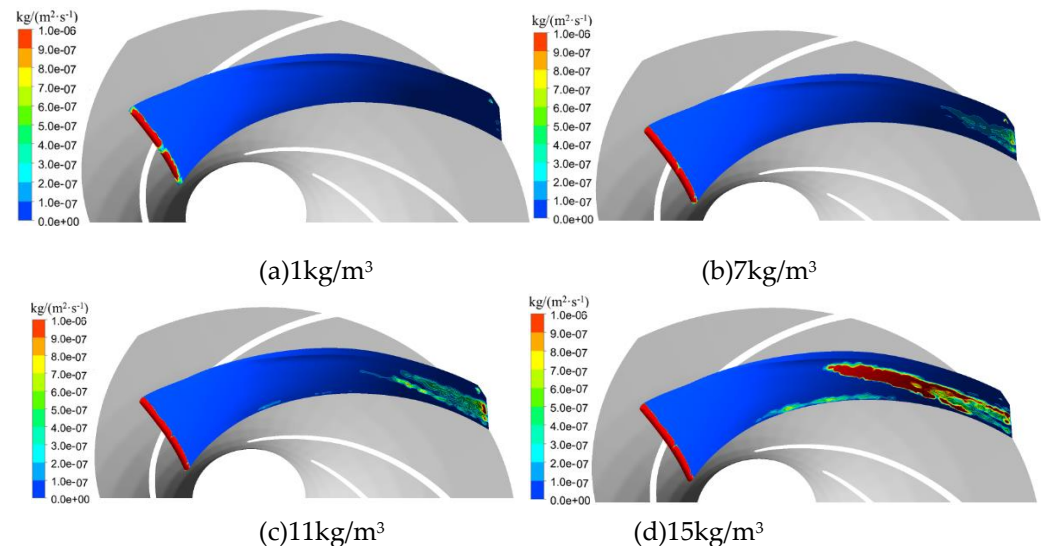


Figure. 19 Erosion rate distribution of single blade with different particle concentrations

To quantitatively analyze the erosion rate with the change of particle concentration, assuming that the pump runs continuously for one year, the change of erosion mass loss at different positions of a single blade with particle concentration is shown in figure 20. The results show that the erosion mass loss at different positions increases with the increase of particle concentration, which indicates that the particle concentration has a great influence on the erosion rate, which is consistent with the previous description. Under the same particle concentration, the erosion mass loss at the leading edge of blade is the largest, and that of blade tail is the smallest. The erosion mass loss at pressure surface is larger than that of suction surface, which is consistent with the particle motion characteristics and erosion distribution described in the previous paper.

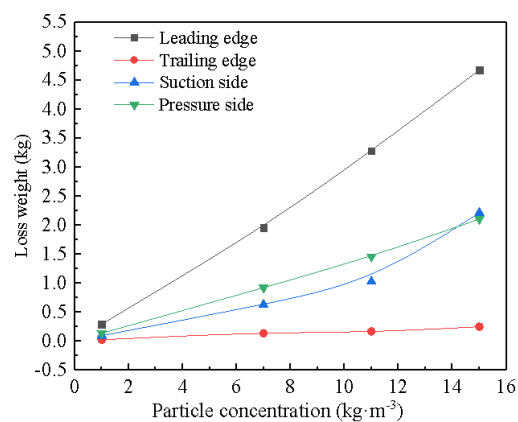


Figure. 20 Change curve of erosion mass loss of single blade with particle concentration

4. Conclusion

Sediment erosion is a major problem affecting the performance and operation life of double suction centrifugal pump. This paper analyzes the particle distribution, particle trajectory and surface erosion in impeller under different flow conditions and different particle concentrations. The conclusions are as follows

(1) The movements and erosion characteristics of particles in impeller under different flow conditions are revealed. The flow structure in the double suction centrifugal pump has a great influence on the erosion in the pump. The flow rate affects the particle trajectory and the uniformity of particle distribution. The more uneven the particle distribution, the more serious the erosion. The greater the relative velocity of the particles, the more serious the erosion on the surface. The erosion of the double-suction centrifugal pump under small flow conditions mainly includes the inflow impact erosion, the friction erosion in the blade channel, the vortex erosion and the impact erosion at the leading edge. The total erosion rate of blade wall is positively correlated with the flow rate, and increases with the increase of flow rate. With the increase of flow rate, the inflow is gradually uniform, and the inflow impact erosion and vortex erosion disappear. The erosion at the impeller is mainly the friction erosion in blade channel and the impact erosion at the leading edge.

(2) The vortex and the secondary flow in the impeller have great influence on particle trajectory. Under the influence of the flow passage vortex in the impeller, the particle trajectory moves from the suction to the pressure surface at the outlet of the impeller. The vortex increases the particle concentration at the exit section of the pressure surface of the blade and intensifies the impact erosion in this area. The particles carried by the local wall-attached vortex rub against the wall of the local vortex region, which aggravates the local friction and erosion. The greater the radius of vortex core, the greater the rotational speed of vortex and the higher the erosion rate. The secondary backflow existing in the blade channel makes it easier for the particles to separate from the carrier current. As the local velocity increases, the particles will also accelerate. This results in a higher impact velocity and an increase in the number of particles hitting the wall of the blade and the rear cover, which in turn leads to serious erosion on the wall.

(3) Since the size of the particle does not change, its force state also does not change. The particle concentration has little influence on the shape and position of erosion, but has obvious influence on the erosion rate and erosion area, which is consistent with the phenomenon of particle movement trajectory. The greater the concentration of particles, the greater the contact area between the particles and the wall, which results in greater erosion on the wall.

Author Contributions: software, XijieSong.; validation, HUili Bi.; formal analysis, Yubin Shen.; investigation, Ning Gu.; resources, Xiaoming Fan.; data curation, XijieSong.; writing-original draft preparation, Xijie Song; writing—review and editing, Zhengwei Wang;. All authors have read and agreed to the published version of the manuscript.” .

Funding: This work was supported by Water conservancy science and technology projects in Ningxia Hui Autonomous Region [DSQZX-KY-01, DSQZX-KY-02], Joint open fund of Tsinghua University Ningxia Yinchuan water network digital water control joint research institute (sklhse-2021-low10). National Natural Science Foundation of China (51876099).

Conflicts of Interest: The authors declare no conflict of interest.

References

- [1] Wang JQ, Jiang WM, Kong FY, et al. Numerical simulation of solid-liquid two-phase turbulent flow and erosion characteristics of centrifugal pump[J].Transactions of the Chinese Society for Agricultural Machinery,2013,44 (11):53-60. (in Chinese)
- [2] Si Huang,Xianghui Su,Guangqi Qiu.Transient numerical simulation for solid-liquid flow in a centrifugal pump by DEM-CFD coupling. Engineering Applications of Computational Fluid M . 2015 (1)
- [3] Yellow River Conservancy Commission of the Ministry of Water Resources Sediment Source and its characteristics. [Online]. (<http://www.yellow.river.gov.cn/hhyl/hhgk/hs/ns>).

- [4] Song X. J., Liu C. Experimental investigation of floor-attached vortex effects on the pressure pulsation at the bottom of the axial flow pump sump[J]. *Renewable Energy*, 2020, 145(12): 2327-2336.
- [5] Song X. J., Liu C. Experimental study of the floor-attached vortices in pump sump using V3V[J]. *Renewable Energy*, 2021, 164(1): 752-766.
- [6] Qian, Zhongdong, Wang, Zhiyuan, Zhang, Kai, Wu, Yuan, Wu, Yulin. Analysis of silt abrasion and blade shape optimization in a centrifugal pump. *Proceedings of the Institution of Mechanical Engineers*. 2014 (5)
- [7] Xu HY, Chen XM, Wang L, et al. A study on motion of solid particles in centrifugal pump impeller[J]. *Fluid Machinery*, 1992, 20(7): 1-6. (in Chinese)
- [8] Liu J, Xu HY, Tang S, et al. Numerical simulation of erosion and particle motion trajectory in centrifugal pump. *Transactions of the Chinese Society for Agricultural Machinery*, 2008, 39(6): 54-59. (in Chinese)
- [9] Xu H Y, Wu Y L, Gao Z Q, et al. Experimental study and numerical analysis of the motion of dilute solid particles in centrifugal pump impellers. *Journal of Hydraulic Engineering*, 1997(9): 12-18. (in Chinese)
- [10] J.K. Edwards, B.S. McLaury, S.A. Shirazi, Modeling solid particle erosion in elbows and plugged tees, *Journal of Energy Resources Technology*. 123(4)(2001)277-284.
- [11] T. Engin, M. Gur, Performance characteristics of a centrifugal pump impeller with running tip clearance pumping solid-liquid mixtures, *J. Fluids Eng.* 123(3)(2001)532-538
- [12] I. Finnie, Erosion of surfaces by solid particles, *Erosion* 3(2)(1960): 87-103.
- [13] G. Grant, W. Tabakoff, Erosion prediction in turbomachinery resulting from environmental solid particles, *J. Aircraft*, 1975, 12(5): 471-478.
- [14] M. Takaffoli, M. Papini, Numerical simulation of solid particle impacts on Al6061-T6 part I: three-dimensional representation of angular particles, *Erosion* 292(2012): 100-110.
- [15] M. Takaffoli, M. Papini, Numerical simulation of solid particle impacts on Al6061-T6 Part II: materials removal mechanisms for impact of multiple angular particles, *Erosion* 296(1-2)(2012)648-655.
- [16] T. Engin, M. Gur, Performance characteristics of a centrifugal pump impeller with running tip clearance pumping solid-liquid mixtures, *J. Fluids Eng.* 123(3)(2001)532-538.
- [17] S. Khurana, V. Goel, G. Singh. Effect of Silt and Jet Diameter on Performance of Turbo Impulse Hydro-Turbine. *ASME 2017 Fluids Engineering Division Summer Meeting* (pp. V01AT03A030), 2017.
- [18] C.I. Walker, A. Goulas. Performance characteristics of centrifugal pumps when handling non-newtonian slurries. *ARCHIVE Proceedings of the Institution of Mechanical Engineers Part A Power and Process Engineering* 1983-1988, vols 197-202, 198(1), 1984, pp. 41-49.
- [19] Zhengjing Shen, Wuli Chu, Xiangjun Li, et al. Sediment erosion in the impeller of a double-suction centrifugal pump—A case study of the Jing tai Yellow River Irrigation Project, China, *Erosion*, 422-423 (2019): 269-279
- [20] A.M. Lospa, C. Dudu, R.G. Ripeanu, A. Dinita, CFD Evaluation of sand erosion erosion rate in pipe bends used in technological installations, *IOP Conf. Ser. Mater. Sci. Eng.* 514 (2019)
- [21] R.E. Vieira, M. Parsi, P. Zahedi, B.S. McLaury, S.A. Shirazi, Sand erosion measurements under multiphase annular flow conditions in a horizontal-horizontal elbow, *Powder Technol.* 320 (2017) 625-636
- [22] D.G. Bhosale, T.R. Prabhu, W.S. Rathod, et al. High temperature solid particle erosion behavior of SS316L and thermal sprayed WC-Cr3C2-Ni coatings, *Erosion*, (2020): 462-463.
- [23] X. Wang, M. Fang, L.C. Zhang, H. Ding, Y.G. Liu, Z. Huang, S. Huang, J. Yang, Solid particle erosion of alumina ceramics at elevated temperature, *Mater. Chem. Phys.* 139(2013): 765-769.
- [24] X. Li, H. Ding, Z. Huang, et al. Solid particle erosion-erosion behavior of SiC-Si3N4 composite ceramic at elevated temperature, *Ceram. Int.* 40(2014)16201-16207.